This article was downloaded by:
On: *25 January 2011*
Access details: *Access Details: Free Access*
Publisher *Taylor & Francis*
Informa Ltd Registered in England and Wales Registered Number: 1072954 Registered office: Mortimer House, 37-41 Mortimer Street, London W1T 3JH, UK

Liquid Crystals

Publication details, including instructions for authors and subscription information:
http://www.informaworld.com/smpp/title~content=t713926090

The effect of polymer chain length on the thermodynamics of acrylate/cyanobiphenyl mixtures

N. Crawford[a]; M. D. Dadmun[a]
[a] Dept. of Chemistry, 323 Buehler Hall, University of Tennessee-Knoxville, TN 37996-1600

To cite this Article Crawford, N. and Dadmun, M. D.(2006) 'The effect of polymer chain length on the thermodynamics of acrylate/cyanobiphenyl mixtures', Liquid Crystals, 33: 2, 195 — 203

To link to this Article: DOI: 10.1080/02678290500446145

URL: http://dx.doi.org/10.1080/02678290500446145

PLEASE SCROLL DOWN FOR ARTICLE

Full terms and conditions of use: http://www.informaworld.com/terms-and-conditions-of-access.pdf

This article may be used for research, teaching and private study purposes. Any substantial or systematic reproduction, re-distribution, re-selling, loan or sub-licensing, systematic supply or distribution in any form to anyone is expressly forbidden.

The publisher does not give any warranty express or implied or make any representation that the contents will be complete or accurate or up to date. The accuracy of any instructions, formulae and drug doses should be independently verified with primary sources. The publisher shall not be liable for any loss, actions, claims, proceedings, demand or costs or damages whatsoever or howsoever caused arising directly or indirectly in connection with or arising out of the use of this material.

Liquid Crystals, Vol. 33, No. 2, February 2006, 195–203

The effect of polymer chain length on the thermodynamics of acrylate/cyanobiphenyl mixtures

N. CRAWFORD and M. D. DADMUN*

Dept. of Chemistry, 323 Buehler Hall, University of Tennessee-Knoxville, TN 37996-1600, USA

(*Received 14 June 2005; accepted 19 September 2005*)

The effect of polymer molecular mass on the phase behaviour and solubility limits of polymer/liquid crystal mixtures is studied for blends of poly(methyl methacrylate) (PMMA) and the small-molecule liquid crystal, 4′-octyl-4-biphenylcarbonitrile (8CB). The phase diagrams from optical microscopy show a limit to the effect of increasing polymer molecular mass. The Flory–Huggins theory (FH) for polymer solutions is used to extract the interaction parameter, χ, from the phase diagrams. The initial FH fits are performed with the assumption that χ is independent of polymer molecular mass, but result in poor correlation to the microscopy data. When χ is allowed to scale with M_w, however, the FH fits are consistent with the limiting molecular mass behaviour. This result represents, to our knowledge, the first time that this scaling behaviour has been observed in polymer/liquid crystal blends. The solubility limit, β, of 8CB in PMMA for each polymer molecular mass is also determined and, when compared with the results of previous studies, support the concept that β is independent of both polymer composition and molecular masses when the polymer molecular mass exceeds *ca.* $5 \times 10^5\,\mathrm{g\,mol^{-1}}$.

1. Introduction

As telecommunication and computing have advanced, the need for new optically active materials remains an important concern, especially for options that minimize power consumption and weight. Fortunately, liquid crystals (LCs) offer a successful option to this need. The liquid crystal display (LCD), for example, has become ubiquitous in the manufacture of such mobile devices as personal digital assistants, notebook computers, and flat-panel televisions [1]. Indeed the use of LCs in displays is projected to become a $7 billion dollar industry by 2005 [2].

The use of LCs, however, is not limited to displays. In recent decades, one class of LC/polymer composites that has shown significant promise in expanding the role of these small molecules to include variable light valves, privacy windows, or even laser resonators, comprises polymer dispersed liquid crystals (PDLCs) [3–8]. These composites consist of LC droplets dispersed throughout a polymer matrix [3, 4]. The polymer acts as a flexible, mechanically strong, optically isotropic structural medium while the birefringent LC provides optical activity [3–5]. Additionally, the polymer matrix provides a means easily to coat the PDLC as a film onto a conducting substrate for the manufacture of electro-optical devices.

In recent years, polymer dispersed liquid crystals have experienced increased demand in the construction of new electro-optical devices. The mechanical strength of the flexible polymer allows PDLCs to be formed into a wide variety of droplet configurations, ranging from the ordered arrays found in holographic diffraction gratings to the random dispersions needed for privacy windows [1–5]. Two critical factors in PDLC performance are the equilibrium morphology of the droplets in the polymer matrix and the amount of residual LC in the polymer matrix, which depend intimately on the phase behaviour and phase separation process of the LC/polymer mixture.

Several theoretical and experimental approaches have emerged from previous research on the phase behavior of PDLCs. Early reports, such as those by Ballauf, and Dorgan and Soane [9, 10] successfully capture the essential features of the upper critical solution temperature (UCST) behaviour of PDLCs through the application of the mean-field thermodynamic theories of Flory, Ronca, and Maier and Saupe to optical microscopy results. Within the same time period the mean-field paradigm was also shown to be useful in the development of calorimetric methods for determining solubility limits of the LC in the matrix. Later studies by Ahn, Kyu, Benmouna, and others established the utility of

---

*Corresponding author. Email: dad@utk.edu

Liquid Crystals
ISSN 0267-8292 print/ISSN 1366-5855 online
http://www.tandf.co.uk/journals
DOI: 10.1080/02678290500446145

optical microscopy, as well as cloud point methods, for the determination of phase behaviour for several different LCs in a variety of matrices [11–14]. From the latter studies, further refinements to the mean-field descriptions resulted in the integration of the Flory–Huggins theory for polymer solutions with the Maier–Saupe–McMillan descriptions of smectic and nematic LCs, an approach that has proved to be quite practical in describing the phase behaviour regardless of LC mesophase.

The polymer molecular mass is a critical parameter that defines the phase separation process and equilibrium phase behaviour of a polymer/LC mixure. However, studies focusing on this subject remain limited in number [8, 12, 13]. Recent work by Gogibus *et al.* observed changes in the phase behaviour of poly(siloxane) blends where increases in polymer molecular mass from 26 000 to 60 000 g mol^{-1} enlarge the immiscibility region of the phase diagram as well as the Flory–Huggins interaction parameter, χ [15]. A more complete study on the effect of molecular mass on polymer/LC phase behaviour is presented by Benmouna *et al.* on linear poly(styrene)/8CB blends with polymer molecular mass ranging from 4 000 to 200 000 g mol^{-1} [11]. The determination of phase diagrams by optical microscopy show dramatic decreases in LC solubility as the poly(styrene) (PS) size increased. Calorimetry was also which was used in these studies to measure the change in the enthalpy of the 8CB liquid crystal phase transitions, used to determine the solubility limits for the LC in these mixtures. The solubility limits in this study indicate a ‘plateau’ with increased PS molecular mass, rather than an expected continual decrease. Moreover, when combined with similar data using poly(methyl methacrylate) (PMMA) as the matrix [13] it appears that the plateau in the solubility limits may be independent of polymer structure.

There still remain significant questions regarding the importance of the polymer molecular mass on the phase behaviour and thermodynamics of polymer/LC blends. Although previous authors have studied the effect of polymer molecular mass on the thermodynamics of LC blends, the range of polymer molecular masses in these studies has been limited to a maximum of 2×10^{5} g mol^{-1}. Since the phase behaviour can still be dramatically altered by doubling or tripling polymer molecular mass beyond 100 000 g mol^{-1} [16], further studies of polymer/LC blends that include molecular masses above 200 000 g mol^{-1} are needed. Another issue that is important in understanding the thermodynamics of polymer/LC mixtures is the arbitrary choices regarding the functional form of the Flory–Huggins interaction parameter, χ, that is extracted from experimental data. Previously, most analyses define the temperature dependence of χ to be $\chi=A+B/T$ and allow A and B to vary to fit data. Clearly A and B have physical origins and their variation in fitting may complicate the interpretation of the thermodynamic analysis and the identification of the important physical parameters that influence the miscibility of polymer/liquid crystal mistures. Finally, the molecular mass dependence of the solubility limits has been proposed to be independent of polymer structure as well as to hold for molecular masses beyond 200 000 g mol^{-1} [11]. The confirmation of this behaviour in polymer matrices with comparable molecular mass ranges but different structure will provide useful evidence to predict the solubility limits for untested polymer matrices.

The work presented in this paper seeks to address these issues by determining the phase behaviour of the polymer/LC mixture, poly(methyl methacrylate) and 4′-octyl-4-biphenylcarbonitrile. Optical microscopy is used to determine the equilibrium phase diagrams of the LC 4′-octyl-4-biphenylcarbonitrile, 8CB, blended with linear poly(methyl methacrylate), PMMA. The weight average polymer molecular mass ranges from 23 000 to 600 000 g mol^{-1}. The microscopy data is analysed using Flory–Huggins theory, where the interaction parameter, χ, of each polymer with the 8CB is extracted, which quantifies the miscibility of the LC in each polymer. Finally, the solubility limits are determined from differential scanning calorimetry (DSC) measurements for the polymer/LC blends studied to compare with previous results.

2. Experimental

2.1. *Materials*

All samples examined by microscopy and DSC comprised poly(methyl methacrylate) (PMMA) and the small molecule liquid crystal 4′-octyl-4-biphenylcarbonitrile (8CB). 8CB and PMMA with higher molecular masses were purchased from Aldrich Chemical Co. and used as received. The lower molecular mass PMMA samples ($M_n\approx23\,000$ and 54 000) were synthesized via atom transfer radical polymerization, ATRP, in the bulk using phenoxy benzene-4,4′-disulphonyl chloride as the initiator and Cu(I) chloride complexed with 2,2′-bipyridine as the catalyst [17]. A list of the molecular mass characteristics of the PMMA samples is given in table 1. The blends were made by dissolving the desired weights of 8CB and PMMA in dichloromethane to give a 50% by mass solution, followed by casting onto a Teflon sheet. After drying for 24 h at 60°C under vacuum, slices from the films were used to make the microscopy and DSC samples.

Table 1. List of polymers used in this study, included are the weight (M_w) and number (M_n) average molecular masses, also the polydispersity indices (PDIs).

Source	M_w	M_n	PDI
ATRP	32200	23200	1.39
	67200	54200	1.24
Aldrich	92700	62000	1.5
	335400	230200	1.46
	614900	258500	2.38

2.2. *Phase diagrams*

Determination of the equilibrium phase diagrams was accomplished by optical microscopy with an Olympus BH-2 microscope. The microscope is equipped with a cross-polarizer for the LC transitions as well as phase-contrast optics to detect the isotropic mixing transitions. The samples cut from the films were mounted on clean glass slides with a Kapton spacer (~25 µm) covered by a glass cover slip. A Mettler FP82HT heating stage with a Mettler FP90 Central Processor controlled the temperature of the sample at a rate of 1°C min^{-1}.

In order to apply Flory–Huggins theory to the microscopy results, the technique employed in this work originates from Benmouna *et al.* and their work with PS/8CB blends [11]. The total free energy, f in equation (1), of the polymer/LC blend consists of two contributions, given as f_i and f_a. The first, f_i, defines the isotropic component due to the mixing,

$$f = f_i + f_a \tag{1}$$

and the second, f_a, describes contributions from the anisotropic behaviour of the LC when below the nematic–isotropic or nematic–smectic transition temperatures. Isotropic mixing of the LC with the polymer, f_i, is given by the Flory–Huggins theory, FH, for polymer solutions while the anisotropic free energy contributions from the coexistence of the polymer with LC in either the nematic or smectic phases, f_a, comes from Maier–Saupe–McMillan theory. It should be noted that the microscopy results presented here are primarily concerned with the mixing of the LC and polymer above the N–I transition. Therefore, our calculations need not include the calculation of f_a from Maier–Saupe–McMillan theory.

The isotropic free energy density for the LC/polymer blends comes from FH, equation (2) where k_B is the Boltzmann constant, and χ is the FH interaction parameter. The first two terms in equation (2) represent the entropy of mixing while the final term yields the enthalpy of mixing.

$$f/k_B T = \phi_1/N_1 \ln\phi_1 + \phi_2/N_2 \ln\phi_2 + \chi\phi_1\phi_2. \tag{2}$$

In FH theory the coexistence curve is determined from the first derivative of the free energy, which corresponds to the chemical potential, given in equation (3).

$$\partial f/\partial\phi_1 = (\ln\phi_1 + 1)/N_1 - (\ln\phi_2 + 1)/N_2 + \chi(\phi_1 + \phi_2). \tag{3}$$

However, before Flory–Huggins can be used to calculate coexistence curves from the microscopy results, two parameters, the effective segment length of the PMMA and the interaction parameter, must be determined from the experimental data.

Determining the effective segment lengths, N_1 and N_2, for both the LC and the polymer is accomplished in the following manner [11, 18]. Since the LC defines the volume of the lattice sites, the segment length of the LC, N_1, is given a value of 1. The segment length of the polymer, N_2, can be found by first obtaining a good fit to a single set of microscopy data, in this case the 90k g mol^{-1} PMMA. The fraction ϕ_{max}, of the LC that corresponds to maximum temperature of the phase diagram, is taken as the critical LC fraction, $\phi_{critical}$, such that $\phi_{max} \approx \phi_{critical}$. The determination of the size of the statistical segment of the PMMA, N_2 is accomplished by using the relationship $\phi_{critical} = N_2^{1/2}/(N_2^{1/2} + N_1^{1/2})$ from Flory–Huggins theory. The value for N_2 is then used to determine the polymer segment size by dividing the molecular mass of the polymer by N_2. The polymer segment size is found to be approximately 10 000 g mol^{-1}, a size that is of the order found in previous studies of PMMA/LC mixtures [10].

The Flory–Huggins interaction parameter, χ, can be determined for each LC/polymer mixture, i.e. as a function of molecular mass from the microscopy data. The determination of χ utilizes the relationship in equation (4).

$$\chi = A + B/T. \tag{4}$$

Here A and B are adjustable parameters while T is the absolute temperature. In polymer/LC blends the phase behaviour typically exhibits an upper critical solution temperature, UCST, where $A<0$, $B>0$ [19–21]. To determine the parameters A and B for a given polymer/LC pair, the critical χ, χ_c is calculated from equation (5), using N_1 and N_2 calculated from the experimental phase diagram.

$$\chi_c = \left(N_1^{-1/2} + N_2^{-1/2}\right)^2 \Big/ 2. \tag{5}$$

Since PMMA, like polystyrene, is a linear polymer, A is initially set equal to −4.5, as was done in a previous study by Benmouna *et al.* for polystyrene/LC blends [11]. B is then calculated using equation (4) and χ_c as well as temperature, T, from microscopy results for the 90k samples.

The coexistence curves are then generated from this data. Initially, χ is assumed to be independent of molecular mass, thus χ, A and B are held constant for all PMMA/LC mixtures, and the coexistence curve of each PMMA/LC mixture is calculated from FH theory. As this method did not accurately describe the experimental data, χ is also allowed to vary with polymer molecular mass. In this procedure, the parameters in equation (4) are determined by determining χ_c from equation (5) for each PMMA molecular mass and the corresponding critical temperature, T_c, from each experimentally determined phase diagram. χ, as described in equation (4), is considered to possess both enthalpic and entropic contributions rather than be a purely enthalpic parameter [20, 22–27]. The B parameter is attributed to the enthalpic contributions of this fitting parameter arising from the exchange energy from inter-/intra-molecular contacts [22]. The entropic term, A, accounts for all other sources of non-combinatorial entropy such as the change in molecular packing that must occur before solution components mix [22]. Since the chemical composition of the matrix remains the same throughout our experiments the exchange energies between 8CB and the PMMA segments should remain the same, hence B is held constant in our calculations. A is allowed to vary, because changing the PMMA molecular mass alters the number of polymer segments; this in turn may alter such factors as the packing of the PMMA and LCs, which would alter the way the solution components pack, altering the non-combinatorial entropy contribution to the mixing. Thus, in accounting for the molecular mass dependence of χ, the value of A is allowed to vary with molecular mass. This analysis allows a more thorough interpretation of the important parameters that influence the thermodynamics of polymer/LC mixtures.

2.3. *Solubility limits*

In the original works by Smith and co-workers, DSC studies of PDLCs found that complete separation of the LC from the polymer matrix never occurs [28–30]. Rather, a percentage of the LC remains trapped within the polymer matrix and acts like a plasticizer. The consequence of the trapped LC is a reduction in the amount of phase-separated LC, a condition that not only affects the potential cost of the PDLC but also the final morphology of the LC droplets. As a result, the determination of the amount of LC that remains miscible in the polymer-rich matrix becomes a fundamentally important parameter to the construction and operation of PDLCs.

Smith *et al.* showed that the enthalpy of the nematic–isotropic (N–I) transition, $\Delta H_{\text{N-I}}$ (per unit mass), for the PDLC decreases linearly with LC content. Since only the phase-separated LC within the matrix contributes to $\Delta H_{\text{N-I}}$, the mass of phase separated LC in the droplets can be determined from an experimentally determined $\Delta H_{\text{N-I}}$. The ratio, P, of the mass of the LC in the droplets to the mass of the total PDLC, can thus be determined as a function of total PDLC composition. If the PDLC were completely phase separated, a plot of P vs. PDLC composition should be a straight line that intersects the x-axis at zero. However, if there remains LC distributed throughout the polymer-rich matrix, this plot will intercept the x-axis at a positive non-zero value that is equal to the amount of LC that remains miscible with the polymer matrix. This value is know as the solubility limit of the LC in the polymer and is denoted by the variable β.

β was determined for all blends studied in this project by DSC using a Mettler-Toledo 821e instrument. Samples from the same films that are used in the microscopy experiments were produed by placing 4–10 mg of the blend into 40 µl aluminum DSC pans. The samples were heated from 25 to 70°C at $1^\circ\text{C}\,\text{min}^{-1}$ repeatedly. Data was collected and analysed only after consecutive runs yielded identical curves. $\Delta H_{\text{N-I}}$ of the LC present in the mixture was obtained for all samples by integrating the N–I transition in the DSC thermogram and normalizing to the total sample mass. The normalized $\Delta H_{\text{N-I}}$ was plotted versus the weight fraction of 8CB in the sample, and the extrapolation of the normalized $\Delta H_{\text{N-I}}$ to zero determined the solubility limit, β, of 8CB.

3. Results

A typical example of the experimentally determined phase diagrams for the PMMA/8CB blends is shown in figure 1 for PMMA with a molecular mass of 92 000. The smectic–nematic as well as the nematic–isotropic transitions for 8CB appear at approximately 32°C and 41°C, respectively, for all blends in this study. The isotropic mixing transition is shown by the upper set of data points in each graph. Comparison of the isotropic mixing data for all PMMA molecular masses studied can be found in figure 2. A steady increase in the mixing temperatures is observed with increasing molecular mass for 32k to 90k, however, between 90k and 600k the change in mixing temperatures becomes minimal.

Flory–Huggins theory is fitted to the microscopy data as described in the experimental section, and these fits are shown in figures 3 and 4. Figure 3 shows the result

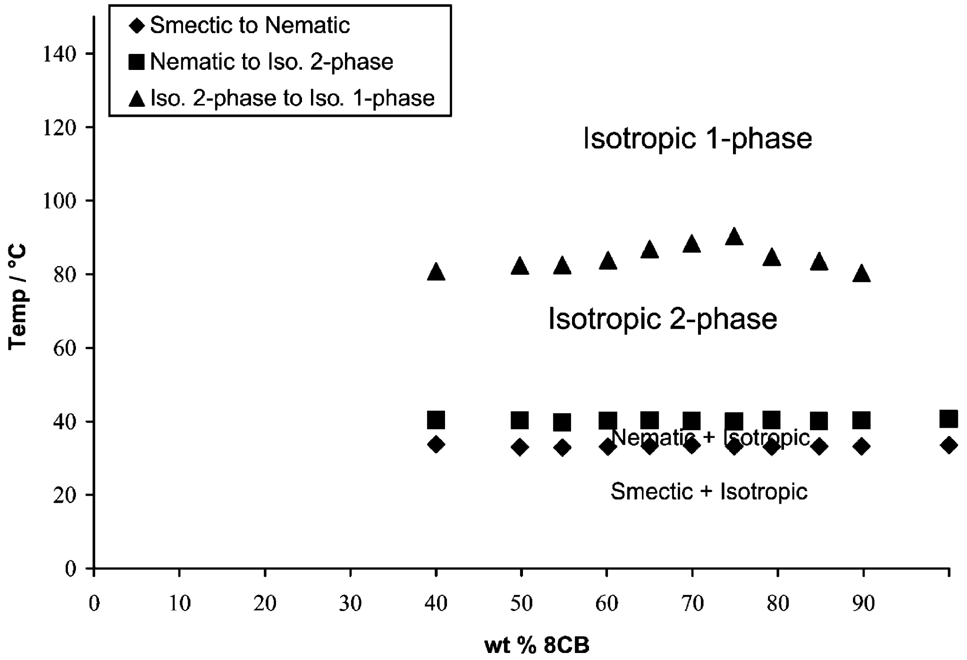

Figure 1. Typical phase diagrams for PMMA/8CB blends, PMMA M_w=92 700 g mol^{-1}; (◆) smectic to nematic transition, (■) nematic to isotropic transition, (▲) isotropic mixing transition.

if χ is held constant for all molecular masses, while figure 4 displays the fits when χ is allowed to vary with polymer chain length. The χ_c values used to create the theoretical coexistence curves are presented in table 2. Note the lack of agreement between the data and the theoretical coexistence curves in figure 3 for all molecular masses other than 90 000. Clearly a χ that is independent of molecular mass does not accurately describe this system. Figure 4, however, presents the fits to FH theory, where χ is allowed to vary with molecular weight [21, 31, 32]. The rationale for adopting the molecular mass dependence of χ in the fits is guided by the fact that there is experimental evidence of a molecular mass dependence of χ [21, 31]. Moreover, by fitting the phase behaviour data of each blend to FH and extracting values of χ, the effect of polymer

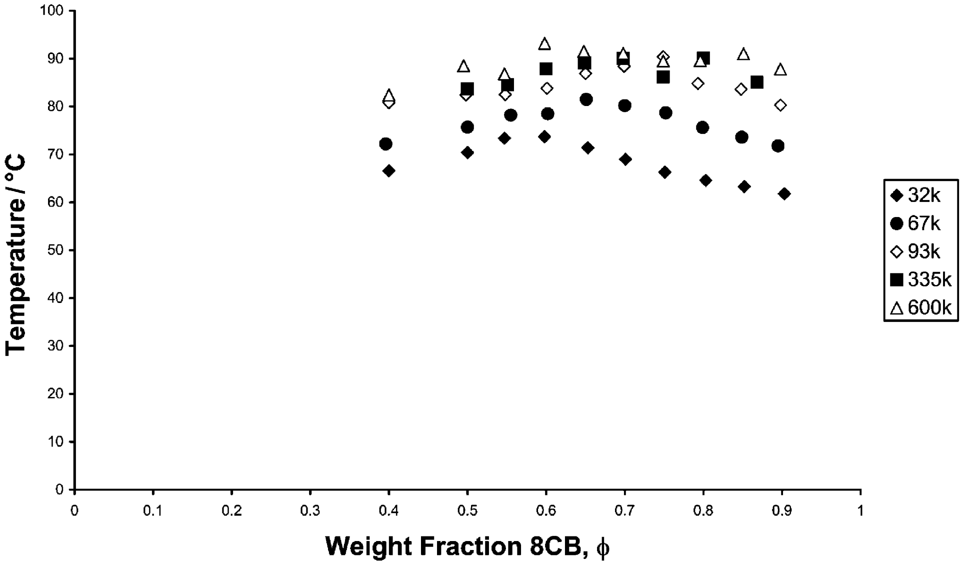

Figure 2. Microscopy data for isotropic mixing of PMMA with 8CB for all PMMA weight average molecular masses; (◆) 32 200, (●) 67 200, (◇) 92 700, (■) 335 000, (△) 614 500 g mol^{-1}.

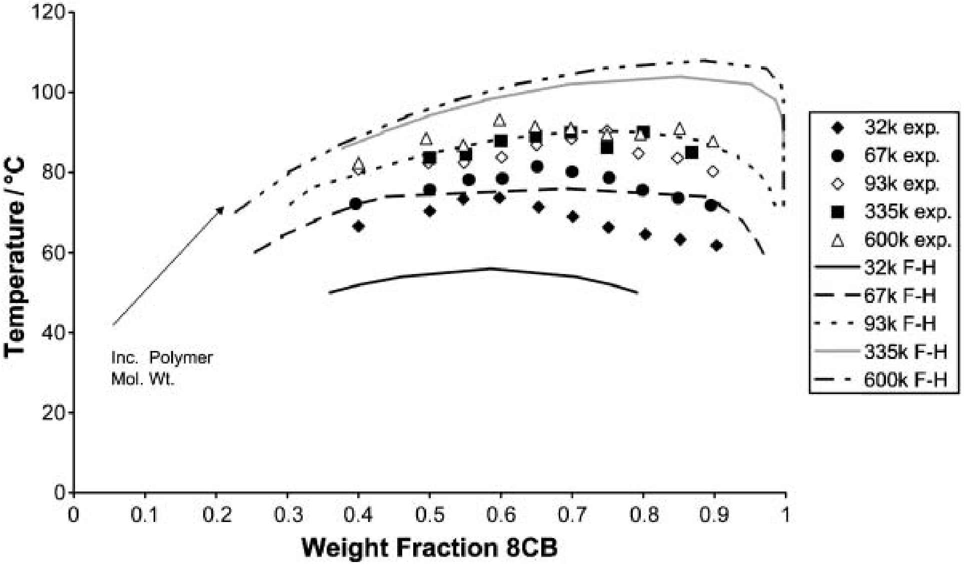

Figure 3. Initial fits of microscopy data for the isotropic mixing transition to FH; χ has no molecular mass dependence; (◆) 32 200, (●) 67 200, (◇) 92 700, (■) 335 000, (△) 614 500 g mol^{-1}.

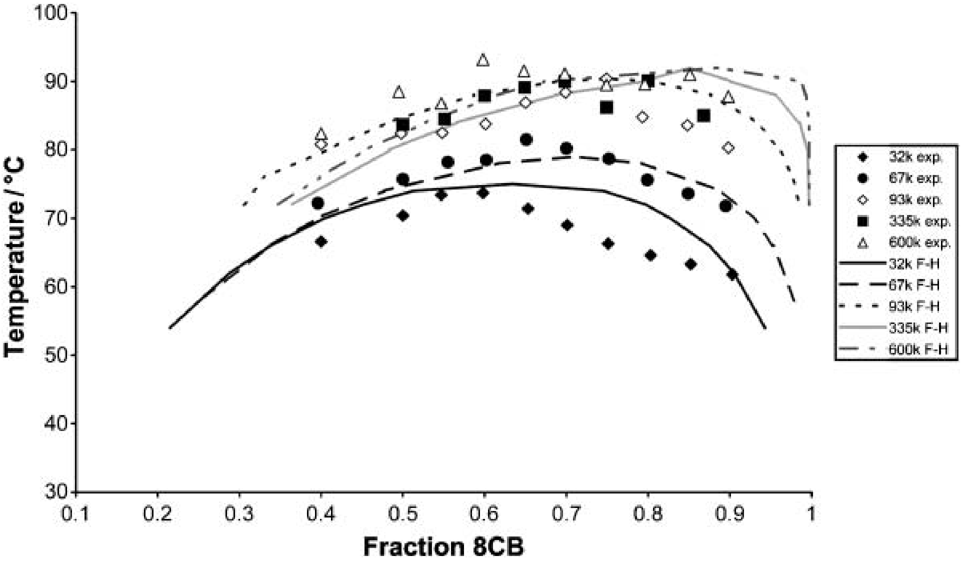

Figure 4. Fits of microscopy data for the isotropic mixing transitions to FH, where χ scales with M_w; (◆) 32 200, (●) 67 200, (◇) 92 700, (■) 335 000, (△) 614 500 g mol^{-1}.

Table 2. Values for the polymer segment lengths, N_2, critical fraction, ϕ_c, and the critical interaction parameter, χ_c, extracted from the microscopy data; effective segment size for N_2 determination *c*. 10 000 g mol^{-1}.

Molecular mass	N_2	ϕ_c	χ_c
32200	3	0.634	1.24
67200	6	0.71	0.992
92700	8	0.749	0.889
335400	33	0.852	0.689
614900	61	0.886	0.636

molecular mass on the phase behaviour can be quantified. This quantification is shown in figure 5, which is a log–log plot of χ vs. molecular mass at 60°C. The overall trend in the scaling of χ in figure 5 indicates that $\chi \sim M_w^{-0.1}$ in this system. Moreover, when χ is allowed to depend on the molecular weight, the FH theory fits the experimental data very well for all PMMA molecular masses.

The solubility limits of 8CB in the polymers studied were determined by DSC and are presented in figures 6

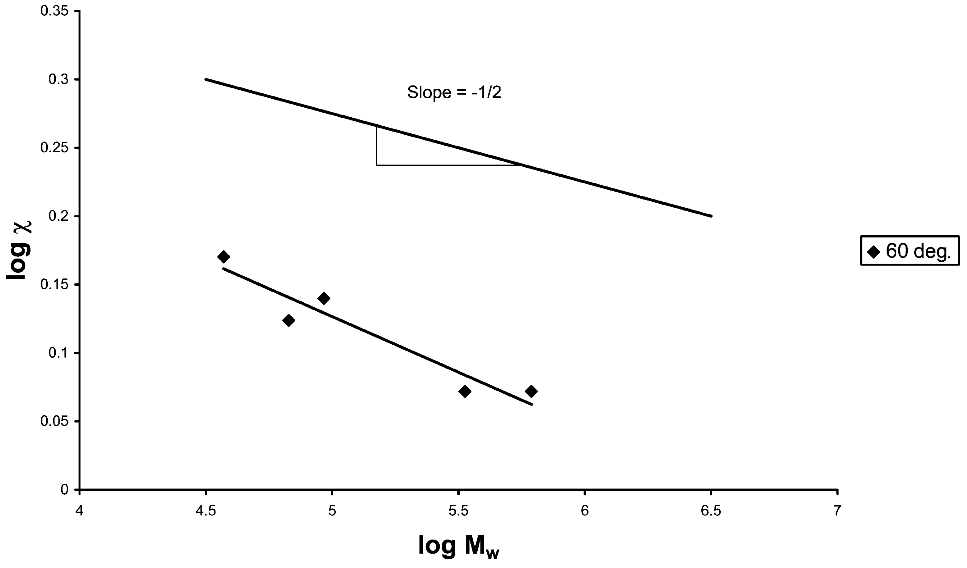

Figure 5. Comparison of the scaling of extracted χ values at 60°C to mean-field prediction of $\sim M_w^{-0.5}$.

and 7. Figure 6 shows typical data quantifying the solubility limit, β, for the blends; this figure displays the data for the blend containing PMMA with 90 000 molecular mass. The x-intercept at $\Delta H_{\text{N-I}}=0$ of these plots provides the solubility limit for 8CB in the PMMA matrix. The data in figure 7 present the molecular mass dependence of β for this study and previous work [11]. This plot indicates that β decreases with increasing molecular mass up to *ca*. 100 000 and then plateaus to an LC fraction around 0.4 for higher molecular mass polymers.

4. Discussion

The data show that as the chain length of a polymer increases, the miscibility of the polymer with a liquid crystal decreases. However, when the molecular mass of poly(methyl methacrylate) becomes larger than ~100 000, which corresponds to a degree of polymerization of about 1 000, a further increase does not significantly change the miscibility curve. This result is the first time such a limit has been observed experimentally for polymer/LC systems.

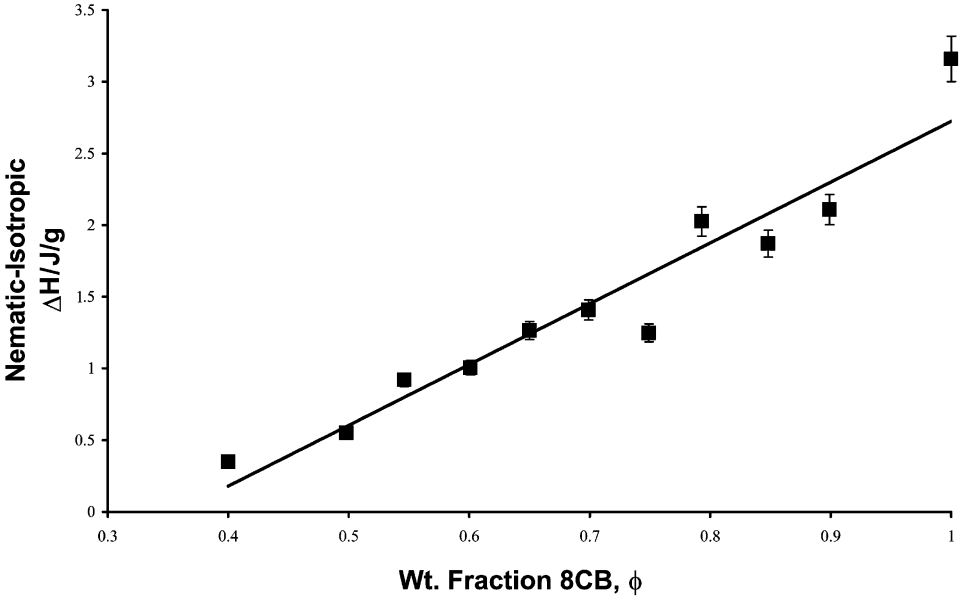

Figure 6. Typical DSC results for $\Delta H_{\text{N-I}}$ used to extrapolate ϕ, PMMA M_w=92 700 g mol^{-1}; x-intercept yields β, the solubility limit.

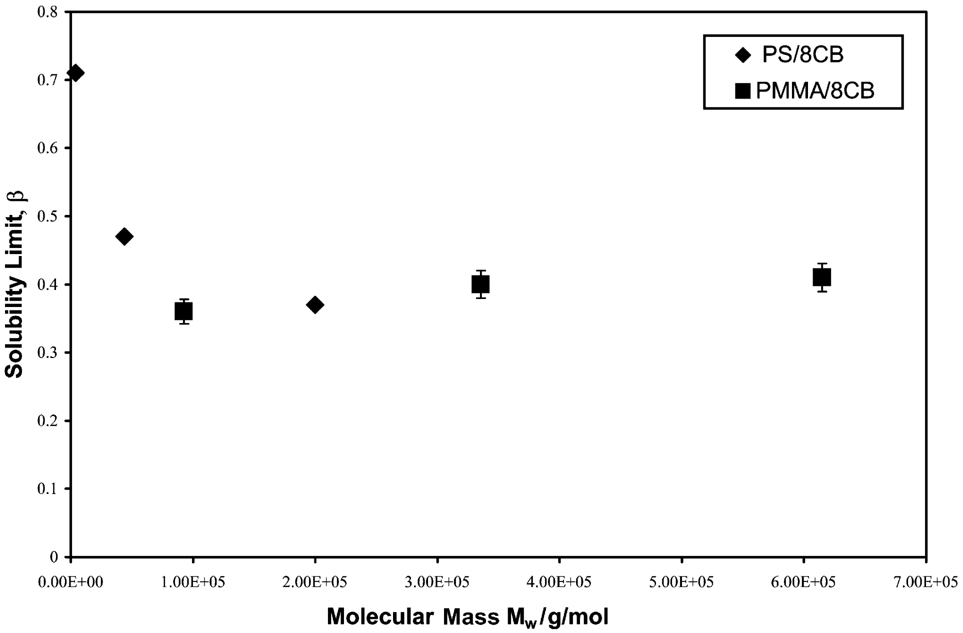

Figure 7. Comparison of solubility limits; (◆) from Benmouna *et al.* for PS/8CB blends, (■) solubility limits from this study.

The extraction of χ from the microscopy data provides a method to quantify this limiting molecular mass behaviour observed in the phase diagrams. χ can be expected to scale with molecular mass, which originates from corrections to FH theory [19, 20, 31–34]. These corrections predict that $\chi \sim M_w^{-0.5}$. However, from figure 7, the experimental data show scaling of $\chi \sim M_w^{-0.1}$. One possible explanation for this dependence is provided by theories that account for the volumetric differences of the LC molecules relative to the polymer segments [25]. The basic framework of the FH model assumes that each lattice site is represented by a uniform volume within the solution, no matter if the site is occupied by polymer segment or LC molecule. For this assumption to hold in our blends, both the PMMA segments and the 8CB molecules would have to occupy similar volumes. However, given the rigidity of the 8CB molecule as compared with the more flexible PMMA segments, such a condition is unlikely. An explanation of the observed scaling behaviour must include a description that retains the essential features of the FH approach but accounts for the deviations arising from structural asymmetry.

Recent studies by Dudowicz *et al.* explore the effect of molecular structure on the scaling behaviour of such FH parameters as critical temperature, T_c, and volume fraction, ϕ_c, by a simplified lattice cluster theory, or SLCT [27]. The 'simplification' in this case is performed by taking the regular lattice cluster theory, a description that corrects the FH free energy of mixing for changes caused by different molecular structures, and imposing high pressure conditions that remove compressibility contributions. In this way the authors are able to isolate the entropic changes arising from the intermolecular packing, as well as make comparisons of the scaling behaviour from their SLCT calculations to the FH predictions.

In this model, $T_c \sim N$, and ϕ_c follows the same relationship stated in the experimental section of this paper. However, the authors find that, in changing the basic molecular shapes, ϕ_c shows a weak dependence on N, but T_c shows several highly complex molecular mass dependences that deviate dramatically from the FH prediction. Since the χ values extracted from microscopy are derived from the critical temperature, shape issues affecting the molecular mass dependence of T_c can lead to deviations in the scaling of χ with M_w.

The molecular mass dependence of the solubility limit, β, for PMMA/8CB blends appears to mesh very well with previous results. Experimental results given in figures 6 and 7 represent, to our knowledge, the first such study performed on PMMA/8CB blends. From the data obtained by DSC, β decreases with increasing PMMA molecular mass to 0.40, and levels off at high polymer molecular mass. In previous work by Benmouna on PS/8CB blends the presence of this plateau is attributed to the formation of a strongly entangled physical network [11]. By extending the data to masses beyond 100k the comparison of our data to the universal curve supports the limiting molecular mass hypothesis. Additionally, the similarity between β values of PS/8CB blends and our PMMA/8CB blends lends further support to the independence of solubility limits from polymer composition.

5. Conclusions

The UCST of a blend of poly(methyl methacrylate) and 8CB increases significantly with polymer chain length if the degree of polymerization of the polymer is less than *ca.* 1 000. Above a DP of 1 000, the UCST barely increases with polymer chain length. This limiting molecular mass dependence is captured quantitatively by allowing the Flory-Huggins interaction parameter, χ, to scale with polymer molecular mass to the -0.1 power. This power law dependence can be explained in terms of the structural differences between the PMMA segments and 8CB molecules. This power law dependence and limiting molecular mass behaviour has not been previously presented in the literature for linear acrylate matrices and, represent an important contribution to the understanding of the impact of polymer molecular mass on the phase behaviour of PDLCs.

The solubility limits, β, of the PMMA/8CB blends are presented. As PMMA molecular mass increases, β reaches a plateau of 40 wt% 8CB, an indication the polymer-rich phases are saturated with LC. Comparison of the results with Benmouna's data strengthens the argument that the solubility limit of an LC in a polymer matrix plateaus for high molecular masses as well as for the universality of this behavior of LC and coiled polymer mixtures.

References

[1] S. Chin. *EBN*, 18 (2003).

[2] J. Markarian. *Chem. Mark. Rep.*, 262 (2002).

[3] P.J. Collings, J.S. Patel. *Handbook of Liquid Crystal Research*. Oxford University Press, New York (1997).

[4] M. Mucha. *Prog. polym. Sci.*, **28**, 837 (2003).

[5] C. Gu, Y. Xu, L. Yisi, J.J. Pan, F. Zhou, H. He. *Opt. Mater.*, **23**, 219 (2003).

[6] T.J. Bunning, L.V. Natarajan, V.P. Tondiglia, R.L. Sutherland. *Ann. Rev. mater. Sci.*, **30**, 83 (2000).

[7] R. Jakubiak, T.J. Bunning, R.A. Vaia, L.V. Natarajan, V.P. Tondiglia. *Adv. Mater.*, **15**, 241 (2003).

[8] P.S. Drzaic. *Liquid Crystal Dispersions*. World Scientific Publishing Co., River Edge, NJ (1995).

[9] M. Ballauff. *Mol. Cryst. liq. Cryst. Lett.*, **4**, 15 (1986).

[10] J.R. Dorgan, D.S. Soane. *Mol. Cryst. liq. Cryst.*, **188**, 129 (1990).

[11] F. Benmouna, A. Daoudi, F. Roussel, L. Leclerq, J. Busine, X. Coqueret, M. Benmouna, B. Ewen, U. Maschke. *Macromolecules*, **33**, 960 (2000).

[12] T. Kyu, C. Shen, H.-W. Chiu. *Mol. Cryst. liq. Cryst.*, **287**, 27 (1996).

[13] W. Ahn, C.Y. Kim, H. Kim, S.C. Kim. *Macromolecules*, **25**, 5002 (1992).

[14] F. Roussel, J. Buisine, U. Maschke, X. Coqueret, F. Benmouna. *Phys. Rev. E*, **62**, 2310 (2000).

[15] N. Gogibus, F. Benmouna, B. Ewen, T. Pakula, X. Coqueret, M. Benmouna, U. Maschke. *J. polym. Sci. B*, **41**, 39 (2003).

[16] A. Stroeks, E. Nies. *Macromolecules*, **23**, 4092 (1990).

[17] E.A. Eastwood, M.D. Dadmun. *Macromolecules*, **35**, 5069 (2002).

[18] F. Benmouna, U. Maschke, X. Coqueret, M. Benmouna. *Macromol. Theory Simul.*, **9**, 215 (2000).

[19] P.C. Hiemenz. *Polymer Chemistry: The Basic Concepts*. Marcel Dekker, Inc., NY (1984).

[20] M.A. van Dijk, A. Wakker. *Polymer Thermodynamics Library,* Vol. 2: Concepts of Polymer Thermodynamics, ChemTec Publishing, Lancaster, PA (1997).

[21] T. Nishi. *J. macromol. Sci.-Phys.*, **B17**, 517 (1980).

[22] R. Koningsveld, L.A. Kleintjens. *Macromolecules*, **4**, 637 (1971).

[23] G. Beaucage, R.S. Stein, R. Koningsveld. *Macromolecules*, **26**, 1603 (1993).

[24] H. Petri, N. Schuld, B.A. Wolf. *Macromolecules*, **28**, 4975 (1995).

[25] N. Schuld, B.A. Wolf. *J. polym. Sci. B*, **39**, 651 (2001).

[26] K.F. Freed, J. Dudowicz. *J. chem. Phys.*, **97**, 2105 (1992).

[27] J. Dudowicz, K.F. Freed, J.F. Douglas. *J. chem. Phys.*, **116** (2002).

[28] G.W. Smith, G.M. Ventouris, L. West. *Mol. Cryst. liq. Cryst.*, **213**, 11 (1992).

[29] G.W. Smith. *Mol. Cryst. liq. Cryst.*, **225**, 113 (1993).

[30] G.W. Smith. *Mol. Cryst. liq. Cryst.*, **241**, 32 (1994).

[31] S. Saeki, N. Kuwahara, M. Nakata, M. Kaneko. *Polymer*, **16**, 445 (1975).

[32] M.D. Ghelson, J.H. Rosdale, F.S. Bates, G.D. Wignall, L. Hansen, K. Almdal. *Phys. Rev. Lett.*, **68**, 2452 (1992).

[33] Z. Sun, L. An, H. Li, Z. Jiang, Z. Wu. *Macromol. Theory Simul.*, **10**, 692 (2001).

[34] S. Konno, S. Saeki, N. Kuwahara, M. Nakata, M. Kaneko. *Macromolecules*, **8**, 799 (1975).